ACCOUNTS of chemical research

pubs.acs.org/accounts Article

Metamorphoses of Cesium Lead Halide Nanocrystals

Published as part of the Accounts of Chemical Research special issue "Transformative Inorganic Nanocrystals".

Stefano Toso, Dmitry Baranov, and Liberato Manna*

Cite This: *Acc. Chem. Res.* 2021, 54, 498−508 Read Online

ACCESS | Metrics & More | Article Recommendations

CONSPECTUS: Following the impressive development of bulk lead-based perovskite photovoltaics, the "perovskite fever" did not spare nanochemistry. In just a few years, colloidal cesium lead halide perovskite nanocrystals have conquered researchers worldwide with their easy synthesis and color-pure photoluminescence. These nanomaterials promise cheap solution-processed lasers, scintillators, and light-emitting diodes of record brightness and efficiency. However, that promise is threatened by poor stability and unwanted reactivity issues, throwing down the gauntlet to chemists.

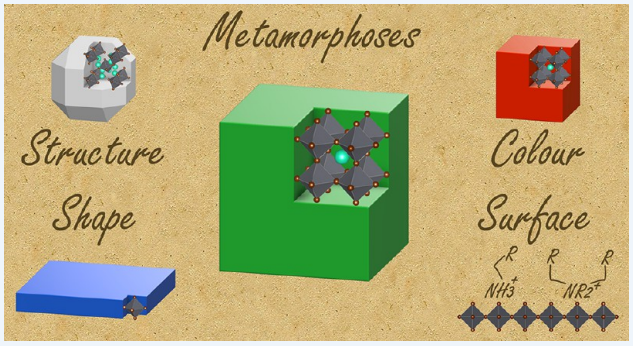

More generally, Cs−Pb−X nanocrystals have opened an exciting chapter in the chemistry of colloidal nanocrystals, because their ionic nature and broad diversity have challenged many paradigms established by nanocrystals of long-studied metal chalcogenides, pnictides, and oxides. The chemistry of colloidal Cs−Pb−X nanocrystals is synonymous with change: these materials demonstrate an intricate pattern of shapes and compositions and readily transform under physical stimuli or the action of chemical agents. In this Account, we walk through four types of Cs−Pb−X nanocrystal metamorphoses: change of structure, color, shape, and surface. These transformations are often interconnected; for example, a change in shape may also entail a change of color.

The ionic bonding, high anion mobility due to vacancies, and preservation of cationic substructure in the Cs−Pb−X compounds enable fast anion exchange reactions, allowing the precise control of the halide composition of nanocrystals of perovskites and related compounds (e.g., $CsPbCl_3 \rightleftarrows CsPbBr_3 \rightleftarrows CsPbI_3$ and $Cs_4PbCl_6 \rightleftarrows Cs_4PbBr_6 \rightleftarrows Cs_4PbI_6$) and tuning of their absorption edge and bright photoluminescence across the visible spectrum. Ion exchanges, however, are just one aspect of a richer chemistry.

Cs−Pb−X nanocrystals are able to capture or release (in short, trade) ions or even neutral species from or to the surrounding environment, causing major changes to their structure and properties. The trade of neutral PbX_2 units allows Cs−Pb−X nanocrystals to cross the boundaries among four different types of compounds: $4CsX + PbX_2 \rightleftarrows Cs_4PbBr_6 + 3PbX_2 \rightleftarrows 4CsPbBr_3 + PbX_2 \rightleftarrows 4CsPb_2X_5$. These reactions do not occur at random, because the reactant and product nanocrystals are connected by the Cs^+ cation substructure preservation principle, stating that ion trade reactions can transform one compound into another by means of distorting, expanding, or contracting their shared Cs^+ cation substructure.

The nanocrystal surface is a boundary between the core and the surrounding environment of Cs−Pb−X nanocrystals. The surface influences nanocrystal stability, optical properties, and shape. For these reasons, the dynamic surface of Cs−Pb−X nanocrystals has been studied in detail, especially in $CsPbX_3$ perovskites. Two takeaways have emerged from these studies. First, the competition between primary alkylammonium and cesium cations for the surface sites during the $CsPbX_3$ nanocrystal nucleation and growth governs the cube/plate shape equilibrium. Short-chain acids and branched amines influence that equilibrium and enable shape-shifting synthesis of pure $CsPbX_3$ cubes, nanoplatelets, nanosheets, or nanowires. Second, quaternary ammonium halides are emerging as superior ligands that extend the shelf life of Cs−Pb−X colloidal nanomaterials, boost their photoluminescence quantum yield, and prevent foreign ions from escaping the nanocrystals. That is accomplished by combining reduced ligand solubility, due to the branched organic ammonium cation, with the surface-healing capabilities of the halide counterions, which are small Lewis bases.

KEY REFERENCES

- Baranov, D.; Caputo, G.; Goldoni, L.; Dang, Z.; Scarfiello, R.; De Trizio, L.; Portone, A.; Fabbri, F.; Camposeo, A.; Pisignano, D.; Manna, L. Transforming colloidal Cs_4PbBr_6 nanocrystals with poly(maleic anhydride-*alt*-1-octadecene) into stable $CsPbBr_3$ perovskite

Received: October 30, 2020
Published: January 7, 2021

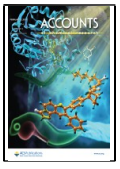

https://dx.doi.org/10.1021/acs.accounts.0c00710
Acc. Chem. Res. 2021, 54, 498−508

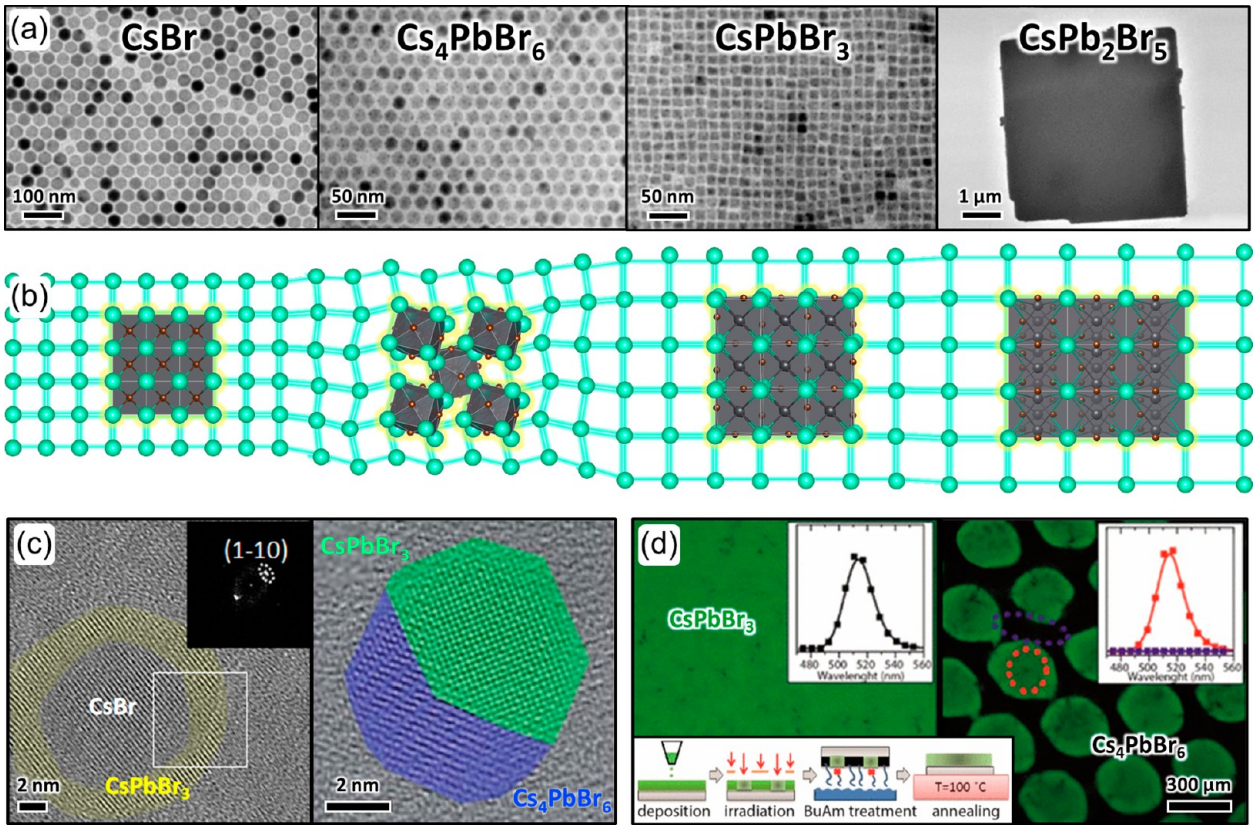

Figure 1. Nanocrystals of different compounds within the Cs−Pb−Br system (a). Side-view of the Cs^+ cation substructure shared among the same compounds (b). Thanks to this common structural feature, nanocrystals can be converted one into another by ion trade reactions exchanging PbX_2. Since ion trade reactions preserve the nanocrystal backbone, their intermediates are epitaxial heterostructures (c). Transformations between Cs−Pb−Br compounds cause instability issues but provide opportunities for applications as well. One example is the templated conversion of a film of $CsPbBr_3$ emissive nanocrystals into nonemissive Cs_4PbBr_6 nanocrystals upon exposure to butylamine vapors, which can be reverted by mild heating (d). Reprinted with permission from refs 1, 10, 13, 15, 18, and 20. Copyright 2020 Royal Society of Chemistry (ref 1) and 2017−2020 American Chemical Society.

emitters through intermediate heterostructures. *Chem. Sci.* **2020**, *11*, 3986−3995.[1] **Change of Structure:** The capture of Cs_4PbBr_6−$CsPbBr_3$ heterostructures during the conversion between Pb-poor and Pb-rich cesium lead halide serves as an elegant illustration of the preservation of Cs^+ substructure principle directing transformations between various Cs−Pb−X compounds.

- Akkerman, Q. A.; D'Innocenzo, V.; Accornero, S.; Scarpellini, A.; Petrozza, A.; Prato, M.; Manna, L. Tuning the Optical Properties of Cesium Lead Halide Perovskite Nanocrystals by Anion Exchange Reactions. *J. Am. Chem. Soc.* **2015**, *137*, 10276−10281.[2] **Change of Color**: The pioneering effort describing ion exchanges in $CsPbX_3$ perovskite nanocrystals that preserve nanocrystal shapes and structures while going from $CsPbCl_3$ to $CsPbBr_3$ to $CsPbI_3$ compositions and spanning the rainbow of visible photoluminescence spectra.
- Imran, M.; Ijaz, P.; Baranov, D.; Goldoni, L.; Petralanda, U.; Akkerman, Q.; Abdelhady, A. L.; Prato, M.; Bianchini, P.; Infante, I.; Manna, L. Shape-Pure, Nearly Monodispersed $CsPbBr_3$ Nanocubes Prepared Using Secondary Aliphatic Amines. *Nano Lett.* **2018**, *18*, 7822−7831.[3] **Change of Shape:** This work paves the way for exclusive shape-control during the perovskite nanocrystal synthesis by means of replacing a primary amine with a secondary amine and suppressing the competition for surface sites.
- Imran, M.; Ijaz, P.; Goldoni, L.; Maggioni, D.; Petralanda, U.; Prato, M.; Almeida, G.; Infante, I.; Manna, L. Simultaneous Cationic and Anionic Ligand Exchange For Colloidally Stable $CsPbBr_3$ Nanocrystals. *ACS Energy Lett.* **2019**, *4*, 819−824.[4] **Change of Surface:** This work shows how a single surfactant quaternary ammonium salt has all the ingredients for a tight surface passivation that boosts the photoluminescence quantum yield (PLQY) to near unity and makes perovskite nanocrystals stable in dispersion even at elevated temperatures.

INTRODUCTION

Cesium lead halide nanocrystals, especially the perovskite ones, have been intensively investigated in the last years thanks to their simple synthesis and appealing optical properties, above all their efficient and spectrally narrow photoluminescence (PL).[5,6] Such properties make this class of materials promising as low-cost optoelectronics components. However, it appeared from the beginning that these materials, particularly in the form of colloidal nanocrystals, suffer from poor stability as they are very reactive toward their surroundings. While this aspect is detrimental for many practical applications, from a chemist's viewpoint it offers the opportunity to investigate, master, and exploit their various possible transformations: these can be structural[1] or compositional,[2] and they can affect the surface[4]

https://dx.doi.org/10.1021/acs.accounts.0c00710
Acc. Chem. Res. 2021, 54, 498−508

or shape,[3] or they can combine all these aspects together. The last 30 years of research on colloidal nanomaterials have provided chemists with an advanced array of tools, and it is no wonder so much has been disclosed since the first report of colloidal perovskite nanocrystals in 2015. In this Account, we provide an overview of transformations affecting cesium lead halide nanocrystals and what we have learned from them.

CHANGING STRUCTURE BY ION TRADE REACTIONS

At first sight, the reactivity of Cs−Pb−X (X = Cl, Br, I, Figure 1a) nanocrystals appears similar to that of binary metal chalcogenide, ME (M = Cd, Pb; E = S, Se, Te), nanocrystals: both classes of materials can exchange ions with their surroundings and modify their composition, with some of the ions migrating in and out of the nanocrystals, while others provide a sturdy backbone to the structure during the process.[7,8] In chalcogenide nanocrystals, anions are bigger than cations and constitute the stable network inside which the small cations migrate.[7] Conversely, the research into lead halide nanostructures revealed that halide vacancies, deformability of the perovskite crystal structure, and lower free energy barriers for vacancy-mediated ionic diffusion underlie the higher mobility of halide anions as compared to Cs^+ cations, despite their similar sizes.[9,10]

The reactivity landscape of Cs−Pb−X nanocrystals is much wider than that of II−VI or IV−VI chalcogenide semiconductor nanocrystals. First, the mobility of ions in Cs−Pb−X compounds is higher than in conventional semiconductors. This stems from the higher ionicity of the metal−halide bonds as compared to metal−chalcogenide ones. For example, the ionicity (difference in Pauling electronegativity) of Cs−X and Pb−X bonds falls in the range of ∼1.9−2.4 and ∼0.8−1.3, respectively, while for (In/Pb/Cd/Zn/Ag/Cu)−(S/Se/Te) pairs the range is ∼0.2−0.9. The higher ionicity of bonds lowers the activation energy for ion migration within the structure, leading to higher reactivity.[11,12] Furthermore, those in the Cs−Pb−X systems are ternary compounds, and this additional level of structural complexity is game-changing. While binary chalcogenide semiconductors are limited to exchanging anions or cations, Cs−Pb−X nanocrystals can also capture or release nominally neutral formula units like PbX_2 and CsX, thus undergoing major changes in their structure and stoichiometry. This makes the concept of ion exchange too limited to adequately capture their reactivity. Instead, Cs−Pb−X nanocrystals are capable of what we will call ion trade reactions, that is, reactions in which a nanocrystal releases or captures species from the environment with a net flux of atoms, while retaining structural relationships between reactant and product nanocrystals. Consistently with this vision, chemical transformations among many Cs−Pb−X compounds have been rationalized with a Cs^+ cubic substructure capturing or releasing PbX_2 units (Figure 1b).[10] The Cs^+ substructure undergoes distortions as it adapts to accept or dispatch ions, without suffering any major changes. A proof is the observation of epitaxial heterostructures between reagent and product compounds, where the Cs^+ sublattice went uninterrupted across the junction. Reports for the CsX → γ-$CsPbX_3$,[13] the Cs_4PbX_6 → γ-$CsPbX_3$,[1] and the γ-$CsPbBr_3$ → $CsPb_2Br_5$ transformations[14] encompassed all the ternary stoichiometries within the Cs−Pb−X system (Figure 1c). It is worth noting that the stoichiometry changes following these ion trade reactions heavily affect the electronic properties of nanocrystals: mild reaction conditions are enough to turn insulators (CsX and Cs_4PbX_6) into direct-bandgap ($CsPbX_3$) or indirect-bandgap ($CsPb_2X_5$) semiconductors.

The concepts of ion trade reaction and Cs^+ substructure preservation give us hints on how a transformation takes place, but they leave aside the reasons for why it takes place. Reactions causing a stoichiometry change necessarily involve the trade of neutral species (CsX or PbX_2); thus they are driven by unbalances in the partition equilibrium of those species between the nanocrystal and its surrounding environment. The simplest case is when the species are directly added or removed from the chemical environment. Examples are reactions driven by the addition of lead-rich compounds such as PbX_2 or Pb-oleate,[13,15] but also the Cs_4PbBr_6 → $CsPbBr_3$ transformation triggered by the sequestration of Cs^+ by Prussian Blue[16] and the concomitant release of Br^- to maintain charge neutrality (= CsBr subtraction). Another driving force is the solubility of neutral species, which can interfere with partition equilibria as well. Almeida et al. rationalized the solubility of PbX_2 in nonpolar solvents as being dependent on the concentrations of $[R\text{-}NH_3]^+$ and $[R\text{-}COO]^-$ ions, which in turn depend on ligands concentration and temperature.[17] Higher temperatures shift the acid−base equilibrium $R\text{-}NH_2 + R\text{-}COOH \rightleftarrows [R\text{-}NH_3]^+ + [R\text{-}COO]^-$ toward the reagents, justifying the inverse solubility of PbX_2 in the reaction. They also demonstrated that conditions favoring high solubility of PbX_2, namely, high ligand concentrations and low temperatures, promote the synthesis of the lead-deficient phase Cs_4PbBr_6. Opposite conditions favor instead the formation of $CsPbBr_3$. Although this study was conducted on direct syntheses, the same principles apply to postsynthetic transformations. One example is the $CsPbBr_3$ → Cs_4PbBr_6 transformation caused by the addition of amines, which increase the solubility of $PbBr_2$ and extract it from the nanocrystals.[18] This transformation also affects solid films when they are exposed to butylamine vapors, and can be used to prepare patterned films of both emissive $CsPbBr_3$ and nonemissive Cs_4PbBr_6 nanocrystals (Figure 1d): this was achieved by irradiating regions of the film with X-rays, which partly cross-linked the organic ligands coating the nanocrystals, creating a barrier against the diffusion of butylamine.

Thermal annealing is another way of triggering ion trade reactions. Palazon et al. demonstrated that heating films of Cs_4PbBr_6 or $CsPbBr_3$ nanocrystals leads to the *in situ* formation of traces of more lead-rich compounds, $CsPbBr_3$ or $CsPb_2Br_5$, respectively.[16,19] Both transformations were rationalized by a ligand-mediated extraction of CsBr, that etches the surface of nanocrystals with the concomitant release of $PbBr_2$. This excess of $PbBr_2$ then intercalates inside the surrounding grains through a solid-state ion trade reaction, driving their transformation to a more lead-rich stoichiometry: Cs_4PbBr_6 turns into $CsPbBr_3$, while $CsPbBr_3$ turns into $CsPb_2Br_5$. These lead-rich phases disappeared in both samples upon annealing above 300 °C. A common explanation can be found in the temperature-driven expulsion of $PbBr_2$ from the crystal lattice, again a solid-state ion trade reaction, which might be related to $PbBr_2$ approaching its melting temperature (373 °C, but lowered in the presence of other species).

CHANGING COLOR BY ION EXCHANGE

So far, we focused on ion trade reactions that induce a change in the nanocrystal stoichiometry. The more familiar ion exchange reactions are a special case of the ion trade class,

https://dx.doi.org/10.1021/acs.accounts.0c00710
Acc. Chem. Res. 2021, 54, 498−508

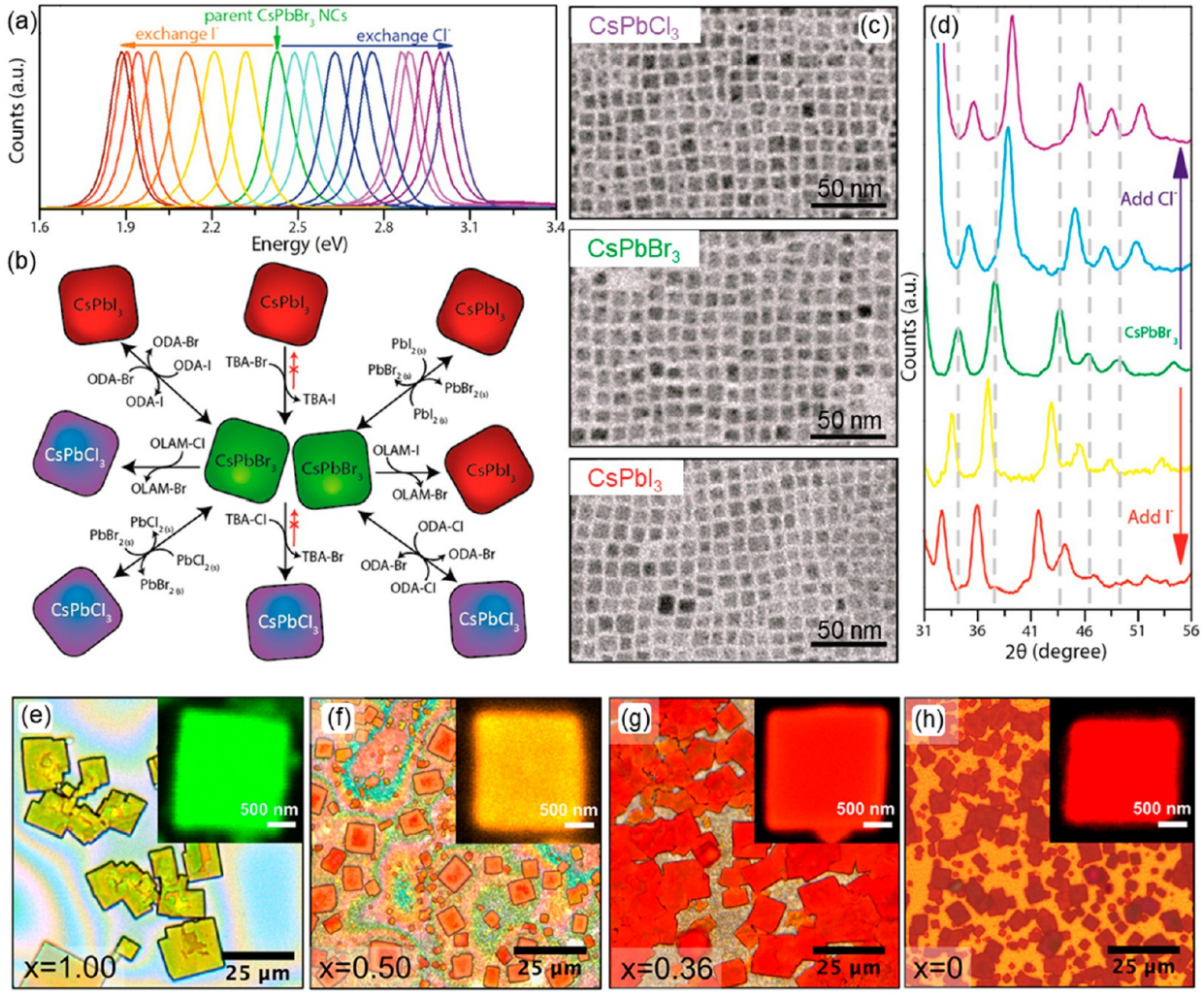

Figure 2. Halide anion exchange in perovskite $CsPbX_3$ nanocrystals allows tuning of their photoluminescence spectrum over a ∼1.2 eV energy range (a). Anion exchange is accessible under ambient conditions through a variety of reagents, such as alkylammonium halide salts (TBA, tetrabutylammonium; ODA, octadecylammonium; OLAM, oleylammonium), or by adding lead salts of the desired halide (b). Throughout the anion exchange, $CsPbX_3$ nanocrystals preserved their shape, size, and perovskite crystal structure, as monitored by TEM (c; fully exchanged $CsPbCl_3$ and $CsPbI_3$ nanocrystals were derived from $CsPbBr_3$ shown in the middle) and XRD (d). The conservative nature of anion exchange was exploited for fabrication of mixed halide $CsPb(I_{1-x}Br_x)_3$ nanocrystal superlattices (e–h, optical microscopy images of the superlattices under white light with insets showing photoluminescence of single superlattices, *x* value indicates the relative Br content with respect to I). Images in panels a–d and e–h are adapted from refs 2 and 25, respectively. Copyright 2015 and 2020 American Chemical Society.

where the net flux of ions between the nanocrystal and its surroundings is null and the stoichiometry and structure remain unchanged. This is a common option for traditional binary chalcogenide semiconductors, and it is available for compounds within the Cs–Pb–X system as well. Reports on anion exchange reactions date back to the first colloidal syntheses of $CsPbX_3$ perovskite nanocrystals by hot injection.[2,21,22] For example, Akkerman et al. achieved fast and complete anion exchange of $CsPbBr_3$ to $CsPbCl_3$ and $CsPbI_3$ nanocrystals (Figure 2a–d) and also provided an early evidence of Cs^+ to methylammonium cation exchange when treating the nanocrystals with methylammonium halides.[2] The anion exchange reactions were found to proceed with both homogeneous (ammonium halides dissolved in toluene) and heterogeneous precursors (powdered PbX_2) and even between pairs of nanocrystals, that is, $CsPbBr_{3(NC)} + CsPb(Cl\text{ or }I)_{3(NC)} \rightarrow CsPb(Br{:}Cl\text{ or }Br{:}I)_{3(NC)}$. Due to the high anion mobility, these reactions easily reached completion and, thanks to the cation substructure preservation, maintained the nanocrystal shape, size, and size distribution. Different from the more drastic reactions involving PbX_2 trade, the preservation of crystal structure and general stoichiometry resulted in a continuous fine-tuning of the optoelectronic properties: on $CsPbX_3$ nanocrystals, ion exchange reactions allowed tuning of the spectral position of the PL anywhere from 3.18 eV ($CsPbCl_3$) to 1.87 eV ($CsPbI_3$) without significant increase in the spectral width as compared to the starting $CsPbBr_3$ nanocrystals (Figure 2a). Moreover, Akkerman et al. noted that, starting from $CsPbBr_3$ nanocrystals, the PLQY after exchange to $CsPbCl_3$ or $CsPbI_3$ dropped to values that were in line with those of as-prepared and $CsPbCl_3$ or $CsPbI_3$ nanocrystals, which are generally less bright than $CsPbBr_3$ nanocrystals.[2] In addition, Mishra et al., when performing a $CsPbBr_3 \rightarrow CsPbCl_3$ anion exchange on nanocrystals and then the inverse $CsPbCl_3 \rightarrow CsPbBr_3$ reaction,[23] noted that the PLQY of the final $CsPbBr_3$ nanocrystals was even higher than that of the initial sample. That result suggests that the creation of additional defects is unlikely. The increase in PLQY at the

https://dx.doi.org/10.1021/acs.accounts.0c00710
Acc. Chem. Res. 2021, 54, 498–508

end of the cycle can be ascribed to a more efficient saturation of the Br^- vacancies on the surface of the final $CsPbBr_3$ nanocrystals compared to the starting ones. Overall, anion exchange reactions do not appear to entail a significant formation of new defects, although further investigations on the topic are needed.

The ability to tune the optoelectronic properties by anion exchange reactions without compromising the morphology and stability of nanocrystals has found many applications to date. For example, Palazon et al.[24] demonstrated a photolithographic approach to produce patterned $CsPbBr_3$ + $CsPb(Cl:Br)_3$ nanocrystal films by masked exposure to HCl vapors. The templating was achieved by cross-linking ligands under X-ray exposure and enabled the preparation of films with regions emitting in different colors. Brennan et al.[25] exploited the morphology-preserving features of anion exchange to prepare mixed-halide $CsPb(Br_xI_{1-x})_3$ nanocrystals with narrow size distribution for self-assembly, starting from monodisperse $CsPbBr_3$ nanocrystals. A series of $CsPb(Br_xI_{1-x})_3$ nanocrystal superlattices with PL tunable from green to red was thus prepared (Figure 2e–h) and their stability under UV illumination was tested. The photoannealing of mixed-halide NC superlattices with a 385 or 470 nm LED light at an incident fluence of $I_{exc} \approx 100$ mW/cm^2 resulted in iodide expulsion and reconversion to $CsPbBr_3$ nanocrystals (albeit with a photobrightening), a process enforced by the iodide photooxidation and I_2 sublimation. Throughout the photo-induced transformation back to $CsPbBr_3$, the nanocrystals preserved their sizes and shapes, both in solution and in superlattices. That observation agrees with the cationic substructure preservation principle.

Anion exchange is not limited to perovskite $CsPbX_3$ nanocrystals. A later work by Akkerman et al.[15] reported anion exchange in the wide-gap Cs_4PbX_6 nanocrystals. Albeit less colorful, the tunability absorption spectrum of Cs_4PbX_6 nanocrystals was demonstrated by tuning the sharp absorption peak from 284 nm (pure Cs_4PbCl_6) to 367 nm (pure Cs_4PbI_6).[15] Here, however, the absorption spectrum for the mixed halide compositions was broader than that for the pure halide compositions. This depends on the molecular-like nature of transitions within individual octahedra. As these octahedra are disconnected in the Cs_4PbX_6 structure, for any mixed composition the absorption spectrum is the convolution of the several optical transitions in the populations of octahedra, differing from one another by both the nature of halide ions surrounding the central Pb^{2+} ion and their mutual spatial arrangement in the coordination environment.

Cation exchange on $CsPbX_3$ nanocrystals has been reported as well, both on the Cs^+ sites and on the Pb^{2+} sites. Cesium can be exchanged with organic cations (typically methylammonium and formamidinium). These exchanges are mostly studied to stabilize the otherwise unstable black $CsPbI_3$ perovskite phase, which shows remarkable photovoltaic performance,[26] and to push their PL further into near-infrared.[27] The case of $Pb^{2+} \rightarrow M^{2+/3+}$ exchange is yet another possibility: postsynthetic exchanges with divalent cations (M = Mn^{2+}, Zn^{2+}, Cd^{2+}, Sn^{2+}), as well as trivalent ones (Bi^{3+}, Ce^{3+}, in these cases at the doping level), have been explored.[28] However, in most cases the process was incomplete, and was generally much slower than anion exchange reactions. Van der Stam et al.[29] rationalized those limitations by a combination of weak driving forces leading to self-limited reactivity and cation diffusion limited kinetics. To overcome this last limitation, they proposed metal halides as precursors, because they dissolve as undissociated MX_2 molecules in nonpolar solvents. In the proposed mechanism, X binds to superficial halide vacancies, securing the cation to the nanocrystal. In addition, the binding energy is enough to break a Pb–X bond, allowing fast $Pb^{2+} \rightarrow M^{2+}$ replacement. This anion-assisted cation exchange has been exploited on other occasions,[30] one remarkable example being the complete $CsPbBr_3 \rightarrow CsSnI_3$ transformation.[31] This interesting case cannot be described by a simple ion exchange and instead fits into the more general category of ion trade reactions. Reacting $CsPbBr_3$ with $SnBr_2$ did not result in any cation exchange:[31] instead, the synergetic replacement of Br for I provided the driving force needed to fully swap lead for tin in the structure. This is a three-player process, where SnI_2 reacted as a neutral species and caused the expulsion of $PbBr_2$, while the Cs^+ cations provided a stable backbone for the structure.

CHANGING COLOR BY SHAPE

Modifying quantum confinement by changing the shape and size of the $CsPbX_3$ nanocrystals allows tuning of their optical properties without changing the nanocrystal composition. This is usually achieved by directly synthesizing cubes with tunable edge lengths,[3,32] nanoplatelets and nanosheets of discrete thicknesses,[33,34] or nanowires.[35] Shape control of $CsPbBr_3$ nanocrystals, and in particular the balance between cube and platelet shapes, again depends on the concentration- and temperature-dependent acid–base equilibrium determined by the balance between $[R\text{-}NH_3]^+$ and $[R\text{-}COO]^-$ species,[17] similarly to the PbX_2 solubility discussed earlier. High acid concentration or low temperature shift the equilibrium toward the oleylamine protonation. In turn, oleylammonium ions, now in high concentrations, start successfully competing with Cs^+ ions on the surface of the growing nanocrystals, a condition that appears to promote the formation of platelets. Lower acid concentrations or higher temperatures instead shift the equilibrium toward unprotonated amines, promoting the formation of cubes. However, the exact reason behind the breaking of the growth symmetry under oleylammonium-rich conditions remains unclear. On the one hand, these conditions might promote the initial formation of monolayer $[oleylammonium]_2PbBr_4$ sheets, consisting of a layer of edge-sharing octahedra sandwiched between two layers of close packed oleylammonium ligands. These sheets then grow thicker as the reaction proceeds. On the other hand, subtle kinetically driven mechanisms might be at work, as that invoked by Riedinger et al. in the formation of CdSe nanoplatelets.[36]

Recent advances in the lead halide perovskite nanocrystal synthesis include the introduction of benzoyl halides as halide source separate from metal ions.[37] That advancement enabled broader experimentation with synthetic conditions such as metal/halide ratio and choice of surfactants used in the synthesis. For example, when oleylamine, which is a primary amine, is replaced with a secondary amine, the shape of the obtained $CsPbBr_3$ nanocrystals is always cubic regardless of temperature and growth conditions.[3] This was explained by considering that secondary ammonium ions bind more weakly to the surface of nanocrystals than primary ammonium ions and hence they cannot act as growth templates. This initial hypothesis was supported by a large body of experimental and computational data that demonstrated a predominance of oleate molecule in the ligand passivation shell of nanocrystals synthesized in the presence of secondary ammonium species. The cube edge length could be controlled by changing the

https://dx.doi.org/10.1021/acs.accounts.0c00710
Acc. Chem. Res. 2021, 54, 498–508

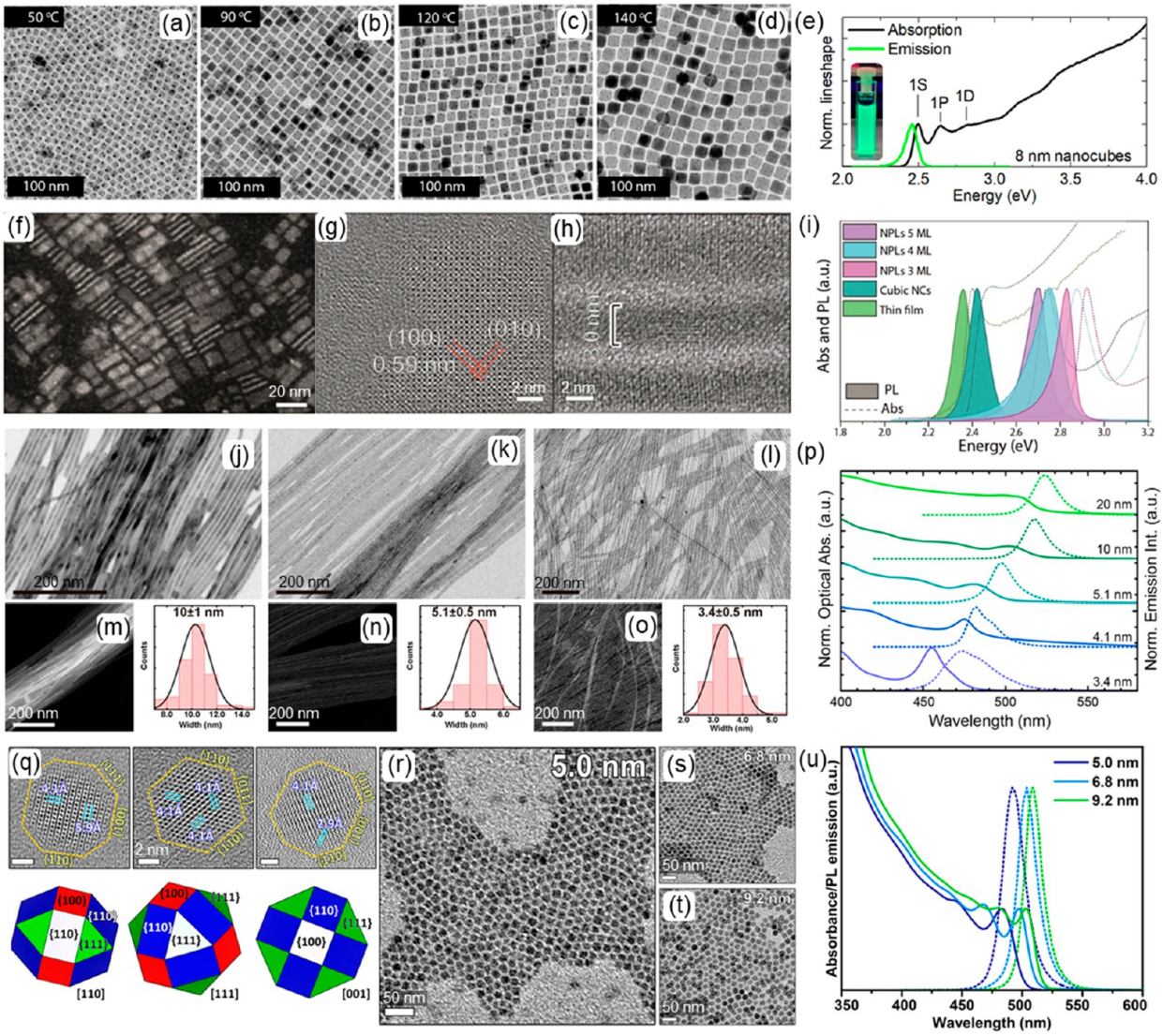

Figure 3. Shape is another dimension of control over optical properties of $CsPbBr_3$ nanocrystals. (a–d) TEM images of nanocubes synthesized with didodecylamine at various temperatures, from ∼6.2 nm at 50 °C to ∼19 nm at 140 °C.[3] Shape-pure nanocubes synthesized with secondary amines display narrow photoluminescence and multiple absorption features in toluene dispersion, indicating the resolution of various electronic transitions (e).[38] (f) Scanning transmission electron microscopy (STEM) image of $CsPbBr_3$ nanoplatelets along with (g, h) high-resolution transmission electron microscopy (HRTEM) images in face and side views, respectively.[33] (i) Comparison of absorption and PL spectra for $CsPbBr_3$ nanoplatelets (NPLs) of various thicknesses and nanocubes.[33] (j–o) TEM and STEM images and thickness histograms for $CsPbBr_3$ nanowires, along with corresponding absorption and PL spectra (p).[35] Using alkylphosphonic acids produces $CsPbBr_3$ nanocrystals with a truncated octahedral shape, as illustrated in (q) HRTEM images and corresponding models.[44] The size of truncated octahedra can be tuned from ∼5 nm to ∼9.2 nm (r–t) by changing reaction time, with corresponding changes in quantum confinement, as tracked by optical absorption and PL (u).[45] Images in panels a–d, f–i, j–p, and q–u are adapted from refs 3, 33, 35, and 45, respectively. Copyright 2018, 2016, 2016, and 2020 American Chemical Society.

chain length of the secondary amine or by changing the reaction temperature while keeping the type of amine fixed. For example, with didodecylamine, the nanocube edge length could be tuned from ∼6.2 nm to ∼19 nm by changing the reaction temperature from 50 to 140 °C (Figure 3a–d). The tunability of the cube edge length enabled fine-tuning of the first exciton peak energy in the range of ∼2.50–2.43 eV, with the corresponding PL maxima in the range of ∼2.46–2.38 eV and narrow line widths (fwhm ∼70–80 meV). The structured absorption spectra of shape-pure $CsPbBr_3$ nanocube samples show multiple electronic transitions (Figure 3e)[38] and attest to the excellent sample uniformity, free of platelets and other morphologies.

A stronger quantum confinement is desirable to push the PL outside the green spectral region toward higher energy and can be achieved by growing ultrathin $CsPbBr_3$ nanoplatelets or nanosheets.[33,39] For example, PL shifts to ∼2.70, 2.76, and 2.83 eV for 5, 4, and 3 monolayer-thick $CsPbBr_3$ nanoplatelets (Figure 3f–i), respectively.[33] Nanowires with a controlled thickness from ∼3 to 20 nm provide another alternative for tuning the quantum confinement in $CsPbBr_3$ nanostructures (Figure 3j–p).[35,40,41] $CsPbBr_3$ nanowires are an interesting case of materials with mixed quantum-confined and bulk-like characteristics, both in dispersions and in films. Thin, blue-emitting $CsPbBr_3$ nanowires (3.5 ± 0.5 nm in diameter) display reversible, concentration-dependent PL shift of up to

https://dx.doi.org/10.1021/acs.accounts.0c00710
Acc. Chem. Res. 2021, 54, 498–508

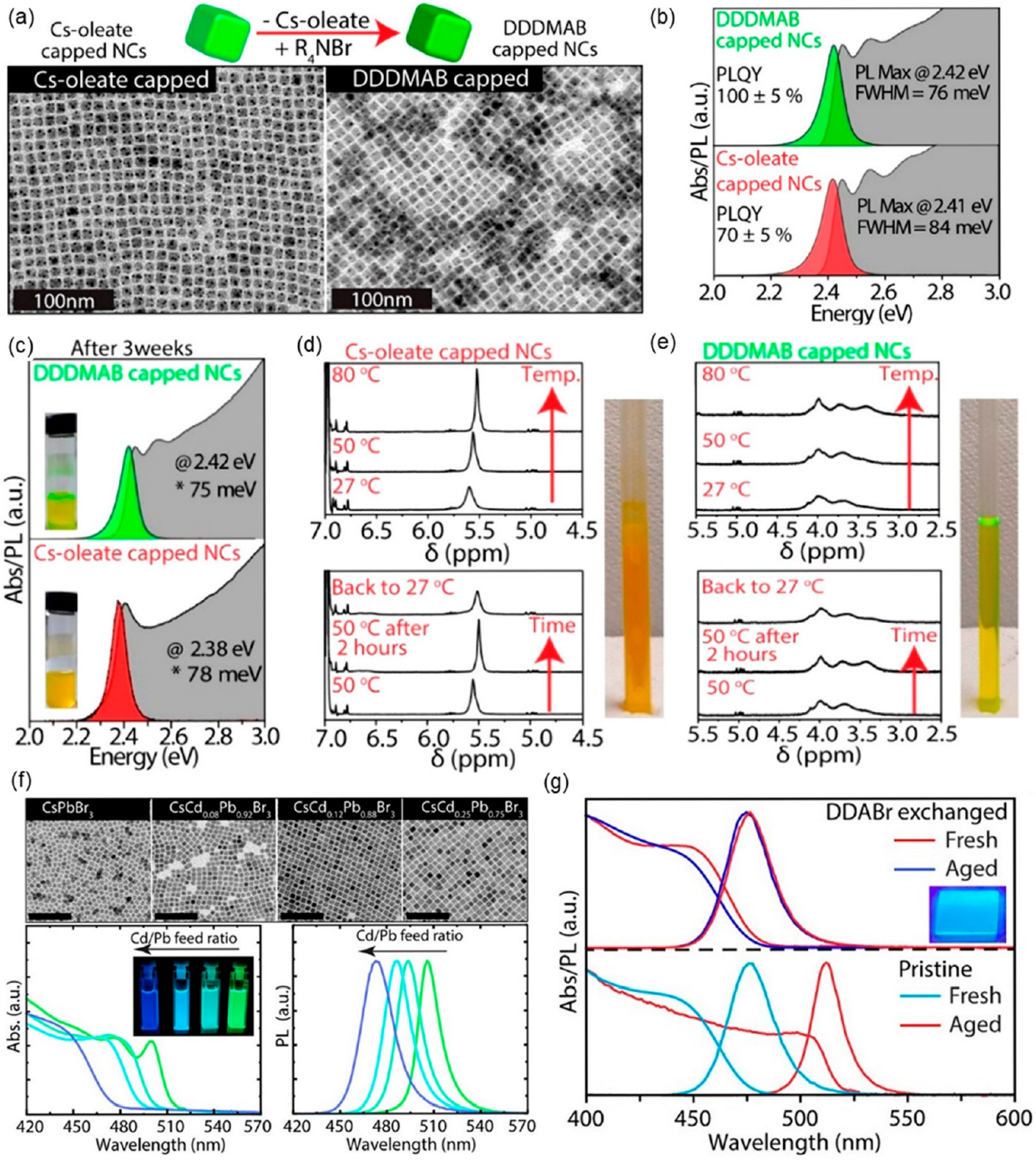

Figure 4. Changing the surface by postsynthesis ligand exchange gives access to brighter and more stable $CsPbBr_3$ nanocrystals. (a) Ligand exchange on originally cesium oleate-capped $CsPbBr_3$ nanocubes (left TEM image) with quaternary ammonium salt that simultaneously accomplished accomplished cation and anion exchange on the surface of the nanocrystals, with minimal distortions to the original nanocrystal shape and size distribution (right TEM image). Optical properties of (b) fresh pre- and postexchange nanocrystals and (c) those aged for 3 weeks. Enhanced thermal stability of surface-exchanged nanocrystals is demonstrated by a cycle of heating the nanocrystal dispersion in an NMR tube for (d) original cesium oleate-capped nanocrystals and (e) exchanged ones. The significantly decreased solvation of quaternary ammonium halide preserves the green-yellow luminescence under ambient light in the case of exchanged nanocrystals, while the original nanocrystals, coated with cesium oleate, begin to aggregate and dim, as captured by photos of the nanocrystal dispersions at the end of the heating experiment. Alloying $CsPbBr_3$ nanocrystals with a variable amount of Cd allows tuning of absorption and emission from blue to green (f). A subsequent surface exchange with DDDMAB stabilizes $Cs(Cd_xPb_{1-x})Br_3$ nanocrystals against Cd expulsion that occurs over time and leads to the loss of blue emission in favor of green one (g). Images in panels a–e and f and g are adapted from refs 4 and 53. Copyright 2019 and 2020 American Chemical Society.

~110 meV to lower energy in toluene dispersions,[42] possibly due to the aggregation-induced relaxation of quantum confinement. Bundles of thick, ~10 nm wide, $CsPbBr_3$ nanowires deposited on glass demonstrate both bulk-like longitudinal exciton diffusion and weak transverse diffusion, indicative of inter-nanowire coupling.[43]

https://dx.doi.org/10.1021/acs.accounts.0c00710
Acc. Chem. Res. 2021, 54, 498–508

More elaborate shape tuning is made possible by resorting to other types of surfactants. Zhang et al. devised a synthesis in which the only surfactants were alkyl phosphonic acids.[44] During the heat-up procedures necessary to dissolve all the reactants, these acids partially underwent condensation reactions and formed phosphonic anhydrides. Indeed, the surface of $CsPbBr_3$ nanocrystals was found to be coated by both hydrogen phosphonates (i.e., deprotonated phosphonic acids) and alkyl phosphonic anhydrides. These ligands bind strongly to facets that are rich in Pb, and these are not only the (010), (101) and $(10\bar{1})$ ones of the orthorhombic perovskite phase but also additional higher index facets. As a result, the nanocrystals had a cuboctahedral shape (Figure 3q). A similar result in terms of shape control was achieved in a more recent work,[45] in which custom-synthesized oleylphosphonic acid was used.[46] The main advantage of using oleylphosphonic acid in lieu of alkyl phosphonic acids is that the former are much more soluble in the nonpolar or moderately polar solvents used to prepare colloidally stable suspensions of nanocrystals, and this has remarkable consequences over the stability of nanocrystals under air: when colloidal suspensions of nanocrystals prepared using alkyl phosphonic acids are exposed to air, the protonation of the hydrogen phosphonates due to moisture should transform them into charge-neutral phosphonic acids, which get detached from the surface of the nanocrystals and, being insoluble, precipitate. This process slowly destabilizes the nanocrystals, which aggregate over time. When instead nanocrystals prepared using oleyl phosphonic acids are exposed to air, moisture may again protonate the surface bound hydrogen phosphonates, which again are transformed into charge-neutral phosphonic acids that detach from the surface. This time, however, these acids are soluble in the solvent used to disperse nanocrystals and can bind back to their surface by losing a proton or even by hydrogen bonding interactions.[45]

The shape transformation of $CsPbBr_3$ nanocrystals can be also achieved by external stimuli. For example, photoannealing of blue-emitting quantum-confined $CsPbBr_3$ nanoplatelets transformed them into green-emitting $CsPbBr_3$ nanobelts with PLQY as high as 65% and amplified spontaneous emission thresholds as low as ~0.25−1 mJ/cm^2 in the solid state.[47] The stages of the photoinduced transformation were captured by TEM, which evidenced an evolution from nanoplatelets, self-assembled face-to-face into stacks, into thicker nanocrystals and belts 30−70 nm wide, over the course of 5 min exposure to a 365 nm LED source. The transformation took advantage of several factors: the strained crystal structure of thin nanoplatelets, their labile surface passivation, and the influence of moisture. The product of photoannealing was a sturdy film of $CsPbBr_3$ nanobelts that did not lose their PL nor did they dissolve upon exposure to toluene or to polar solvents (methanol, ethanol, isopropanol). The increased brightness and stability of the $CsPbBr_3$ nanobelts was exploited to fabricate green-emitting LEDs.

CHANGING SURFACE FOR ENHANCED STABILITY AND PERFORMANCE

The surface chemistry of $CsPbX_3$ nanocrystals is a key to their stability and improvement of optical properties.[48] These nanocrystals can be represented by a formula consisting of [nanocrystal core], (inner shell) and {outer shell}, i.e., $[CsPbX_3](PbX_2)\{AX\}$, where A stands for a cationic ligand (Cs^+, oleylammonium, etc.).[49,50] The stability of nanocrystals in solution is determined by a balance of three interactions: between $[CsPbX_3](PbX_2)$ and {AX}, between $[CsPbX_3]$-(PbX_2) and the solvent, and between {AX} and the solvent. Due to the ionic nature of those nanocrystals, the interactions between $[CsPbX_3](PbX_2)$ and {AX} are of electrostatic nature, with binding energies in the ~41−51.3 kcal/mol range, as calculated from DFT for various ligands (zwitterionic sulfobetaine, cesium oleate, primary and quaternary ammonium halides).[4,32,51] Therefore, the colloidal stability of $CsPbX_3$ in a solvent is dominated by the solvation of the {AX} species. For example, the shape-pure nanocubes discussed earlier carry cesium oleate on their surface, and when dispersed in toluene, they aggregate and react with air and moisture over time, with degradation of their optical properties and loss of PLQY.[3,52] Imran et al. discovered that the addition of quaternary ammonium salts, exemplified by didodecyldimethylammonium bromide (DDDMAB), triggers a simultaneous surface cation and anion exchange (Figure 4a): $[CsPbBr_3](PbBr_2)\{Cs^+\ oleate^-\} + R_2R'_2N^+Br^-_{(solv)} \rightarrow [CsPbBr_3](PbBr_2)\{R_2R'_2N^+\ Br^-\} + Cs\text{-}oleate_{(solv)}$. The shelf life at room temperature of the resulting DDDMAB-treated samples improved significantly as compared to Cs-oleate capped ones (Figure 4b,c). Also, the DDDMAB treatment boosted the PLQY from around 50% to over 90% and made the nanocrystals colloidally stable up to 80 °C in toluene (Figure 4d,e).[4] The good solvation of Cs-oleate in toluene as compared to the poor solvation of DDDMAB is the reason behind the enhanced properties of DDDMAB-capped nanocrystals.

Proper surface passivation was also found to have a key role in stabilizing blue-emitting $CsPb_{1-x}Cd_xBr_3$ alloyed nanocrystals:[53] when part of the Pb^{2+} ions in $CsPbBr_3$ is replaced by Cd^{2+} ions, the structure of the nanocrystals changes from orthorhombic to cubic, and the band gap widens (Figure 4f). As-synthesized, these nanocrystals expel Cd^{2+} ions (and Br^- ions, to maintain charge neutrality) over time, and their emission color shifts to green in a few days. Replacing their native surface ligands with quaternary ammonium bromide ligand pairs prevented the loss of Cd^{2+} ions (and boosted the PLQY). Here, again, DDDMAB was particularly effective. This behavior was rationalized by assuming that surface bromide vacancies are likely facilitating the expulsion of Cd^{2+} ions. When such vacancies are saturated, by coating the nanocrystal surface with ammonium bromide ligand pairs, the loss of Cd^{2+} ions is prevented and the nanocrystals preserve their blue emission over time (Figure 4g).

CONCLUDING REMARKS

In this Account, we have discussed various transformations of cesium lead halide nanocrystals. The diversity of structures, stoichiometries, morphologies, and surfaces in these materials and their inherently fast reactivity produce a broad spectrum of dynamic properties. Given the highly tunable chemistry of cesium lead halide nanocrystals, a common strategy is to obtain a well-defined material (i.e., a nanocrystal with specific structure, size, shape, and passivation) with optimized properties and then fight against their tendency toward reactivity, in order to preserve such properties. This, however, requires a good comprehension of the transformations themselves. From our experience, there are three lessons that come to aid for that. First, the preservation of the Cs^+ cation substructure limits the range of structures among which nanocrystals can transform. Second, the reactivity pathways in

https://dx.doi.org/10.1021/acs.accounts.0c00710
Acc. Chem. Res. 2021, 54, 498−508

the Cs−Pb−X system can be described based on ion trade reactions, which unify stoichiometry-changing and stoichiometry-preserving transformations (i.e., ion exchanges) and account for peculiar behaviors such as anion-assisted cation exchange reactions. Third, the competition between nanocrystal core and environment for the affinity with passivating ligands and the competition between ligands for the surface sites determine the nanocrystal shape during synthesis and the sample stability.

As our understanding of these principles improves, we expect that the reactivity of cesium lead halide nanocrystals will increasingly turn from a challenge to an opportunity. For example, mixing of all three halides (Cl, Br, and I) inside individual Cs−Pb−X nanocrystals leads to the formation of Ruddlesden−Popper defect planes that effectively slice the crystal into separate crystallographic domains.[54] Compositional tuning of those domains may result in a series of strongly quantum-confined wells, potentially enabling us to engineer electron relaxation cascades in individual nanocrystals. Furthermore, a slight doping of mixed $CsPb(I_{1-x}:Br_x)_3$ nanocrystals with chloride may lead to their stabilization against halide segregation under illumination, as was demonstrated in bulk.[55] That coupled together with polymer-enhanced surface chemistry will likely deliver color-tunable and photostable single photon emitters.[56] On a broader perspective, knowing how nanocrystals transform can help prevent or exploit such transformations. For example, halide migration can probably be halted in compounds with mixed covalent/ionic bonding such as chalcohalides[57] or metal−halide compounds in which the formation energy of halide vacancies is high. Growing a shell even a few layers thick of such materials on halide perovskite nanocrystals might prevent them from undergoing anion exchange and other unwanted reactions.

AUTHOR INFORMATION

Corresponding Author

Liberato Manna − *Department of Nanochemistry, Istituto Italiano di Tecnologia, 16163 Genova, Italy;* orcid.org/0000-0003-4386-7985

Authors

Stefano Toso − *Department of Nanochemistry, Istituto Italiano di Tecnologia, 16163 Genova, Italy; International Doctoral Program in Science, Università Cattolica del Sacro Cuore, 25121 Brescia, Italy*

Dmitry Baranov − *Department of Nanochemistry, Istituto Italiano di Tecnologia, 16163 Genova, Italy;* orcid.org/0000-0001-6439-8132

Complete contact information is available at: https://pubs.acs.org/10.1021/acs.accounts.0c00710

Notes

The authors declare no competing financial interest.

Biographies

Stefano Toso was born in 1994 in Genova, Italy, and received his Laurea Degree in Chemistry from the University of Genova in 2018. He is currently a Ph.D. student at the Italian Institute of Technology (IIT) under the supervision of Prof. Manna and part of the International Ph.D. program involving Università Cattolica del Sacro Cuore (Italy) and University of Notre Dame (USA). Stefano specializes in the preparation and structural characterization of novel colloidal nanocrystals and nanocrystal superlattices.

Dmitry Baranov was born in 1986 in Obninsk, Russia, and received his Diploma in Chemistry from the Higher Chemical College of Russian Academy of Sciences in Moscow in 2008, M.Sc. from the University of Chicago in 2011, and a Ph.D. from the University of Colorado—Boulder in 2017. He then joined NACH-IIT as a postdoctoral researcher and then as Marie Skłodowska-Curie Individual Fellow to study energy transfer in nanocrystal assemblies in 2018−2020. Currently, he studies collective optical properties in superlattices of lead halide perovskite nanocrystals.

Liberato Manna was born in 1971 in Barquisimeto, Venezuela, and received his Laurea Degree in Chemistry from the University of Bari in 1996 and his Ph.D. degree in Chemistry from the same University in 2001. Currently, he is a Senior Researcher and Deputy Director at IIT, with expertise in synthesis and structural and optical characterization of nanoscale materials. Recent research efforts of his group are focused on the discovery and development of size-, shape- and composition-control of metal halide nanocrystals.

REFERENCES

(1) Baranov, D.; Caputo, G.; Goldoni, L.; Dang, Z.; Scarfiello, R.; De Trizio, L.; Portone, A.; Fabbri, F.; Camposeo, A.; Pisignano, D.; Manna, L. Transforming colloidal Cs_4PbBr_6 nanocrystals with poly(maleic anhydride-alt-1-octadecene) into stable $CsPbBr_3$ perovskite emitters through intermediate heterostructures. *Chem. Science* **2020**, *11*, 3986−3995.

(2) Akkerman, Q. A.; D'Innocenzo, V.; Accornero, S.; Scarpellini, A.; Petrozza, A.; Prato, M.; Manna, L. Tuning the Optical Properties of Cesium Lead Halide Perovskite Nanocrystals by Anion Exchange Reactions. *J. Am. Chem. Soc.* **2015**, *137*, 10276−10281.

(3) Imran, M.; Ijaz, P.; Baranov, D.; Goldoni, L.; Petralanda, U.; Akkerman, Q.; Abdelhady, A. L.; Prato, M.; Bianchini, P.; Infante, I.; Manna, L. Shape-Pure, Nearly Monodispersed $CsPbBr_3$ Nanocubes Prepared Using Secondary Aliphatic Amines. *Nano Lett.* **2018**, *18*, 7822−7831.

(4) Imran, M.; Ijaz, P.; Goldoni, L.; Maggioni, D.; Petralanda, U.; Prato, M.; Almeida, G.; Infante, I.; Manna, L. Simultaneous Cationic and Anionic Ligand Exchange For Colloidally Stable $CsPbBr_3$ Nanocrystals. *ACS Energy Lett.* **2019**, *4*, 819−824.

(5) Akkerman, Q. A.; Rainò, G.; Kovalenko, M. V.; Manna, L. Genesis, challenges and opportunities for colloidal lead halide perovskite nanocrystals. *Nat. Mater.* **2018**, *17*, 394−405.

(6) Shamsi, J.; Urban, A. S.; Imran, M.; De Trizio, L.; Manna, L. Metal Halide Perovskite Nanocrystals: Synthesis, Post-Synthesis Modifications, and Their Optical Properties. *Chem. Rev.* **2019**, *119*, 3296−3348.

(7) Jain, P. K.; Amirav, L.; Aloni, S.; Alivisatos, A. P. Nanoheterostructure Cation Exchange: Anionic Framework Conservation. *J. Am. Chem. Soc.* **2010**, *132*, 9997−9999.

(8) Luther, J. M.; Zheng, H.; Sadtler, B.; Alivisatos, A. P. Synthesis of PbS Nanorods and Other Ionic Nanocrystals of Complex Morphology by Sequential Cation Exchange Reactions. *J. Am. Chem. Soc.* **2009**, *131*, 16851−16857.

(9) Lai, M.; Obliger, A.; Lu, D.; Kley, C. S.; Bischak, C. G.; Kong, Q.; Lei, T.; Dou, L.; Ginsberg, N. S.; Limmer, D. T.; Yang, P. Intrinsic anion diffusivity in lead halide perovskites is facilitated by a soft lattice. *Proc. Natl. Acad. Sci. U. S. A.* **2018**, *115*, 11929−11934.

(10) Toso, S.; Baranov, D.; Manna, L. Hidden in Plain Sight: The Overlooked Influence of the Cs^+ Substructure on Transformations in Cesium Lead Halide Nanocrystals. *ACS Energy Lett.* **2020**, *5*, 3409−3414.

(11) Mizusaki, J.; Arai, K.; Fueki, K. Ionic Conduction of the Perovskite-Type Halides. *Solid State Ionics* **1983**, *11*, 203−211.

https://dx.doi.org/10.1021/acs.accounts.0c00710
Acc. Chem. Res. 2021, 54, 498−508

(12) Eames, C.; Frost, J. M.; Barnes, P. R. F.; O'Regan, B. C.; Walsh, A.; Islam, M. S. Ionic Transport in Hybrid Lead Iodide Perovskite Solar Cells. *Nat. Commun.* **2015**, *6*, 7497.
(13) Shamsi, J.; Dang, Z.; Ijaz, P.; Abdelhady, A. L.; Bertoni, G.; Moreels, I.; Manna, L. Colloidal CsX (X = Cl, Br, I) Nanocrystals and Their Transformation to $CsPbX_3$ Nanocrystals by Cation Exchange. *Chem. Mater.* **2018**, *30*, 79−83.
(14) Huang, Z.-P.; Ma, B.; Wang, H.; Li, N.; Liu, R.-T.; Zhang, Z.-Q.; Zhang, X.-D.; Zhao, J.-H.; Zheng, P.-Z.; Wang, Q.; Zhang, H.-L. In Situ Growth of 3D/2D ($CsPbBr_3$/$CsPb_2Br_5$) Perovskite Heterojunctions toward Optoelectronic Devices. *J. Phys. Chem. Lett.* **2020**, *11*, 6007−6015.
(15) Akkerman, Q. A.; Park, S.; Radicchi, E.; Nunzi, F.; Mosconi, E.; De Angelis, F.; Brescia, R.; Rastogi, P.; Prato, M.; Manna, L. Nearly Monodisperse Insulator Cs_4PbX_6 (X = Cl, Br, I) Nanocrystals, Their Mixed Halide Compositions, and Their Transformation into $CsPbX_3$ Nanocrystals. *Nano Lett.* **2017**, *17*, 1924−1930.
(16) Palazon, F.; Urso, C.; De Trizio, L.; Akkerman, Q.; Marras, S.; Locardi, F.; Nelli, I.; Ferretti, M.; Prato, M.; Manna, L. Postsynthesis Transformation of Insulating Cs_4PbBr_6 Nanocrystals into Bright Perovskite $CsPbBr_3$ through Physical and Chemical Extraction of CsBr. *ACS Energy Lett.* **2017**, *2*, 2445−2448.
(17) Almeida, G.; Goldoni, L.; Akkerman, Q.; Dang, Z.; Khan, A. H.; Marras, S.; Moreels, I.; Manna, L. Role of Acid-Base Equilibria in the Size, Shape, and Phase Control of Cesium Lead Bromide Nanocrystals. *ACS Nano* **2018**, *12*, 1704−1711.
(18) Palazon, F.; Almeida, G.; Akkerman, Q. A.; De Trizio, L.; Dang, Z.; Prato, M.; Manna, L. Changing the Dimensionality of Cesium Lead Bromide Nanocrystals by Reversible Postsynthesis Transformations with Amines. *Chem. Mater.* **2017**, *29*, 4167−4171.
(19) Palazon, F.; Dogan, S.; Marras, S.; Locardi, F.; Nelli, I.; Rastogi, P.; Ferretti, M.; Prato, M.; Krahne, R.; Manna, L. From $CsPbBr_3$ Nano-Inks to Sintered $CsPbBr_3$−$CsPb_2Br_5$ Films via Thermal Annealing: Implications on Optoelectronic Properties. *J. Phys. Chem. C* **2017**, *121*, 11956−11961.
(20) Ruan, L.; Shen, W.; Wang, A.; Xiang, A.; Deng, Z. Alkyl-Thiol Ligand-Induced Shape - and Crystalline Phase-Controlled Synthesis of Stable Perovskite-Related $CsPb_2Br_5$ Nanocrystals at Room Temperature. *J. Phys. Chem. Lett.* **2017**, *8*, 3853−3860.
(21) Protesescu, L.; Yakunin, S.; Bodnarchuk, M. I.; Krieg, F.; Caputo, R.; Hendon, C. H.; Yang, R. X.; Walsh, A.; Kovalenko, M. V. Nanocrystals of Cesium Lead Halide Perovskites ($CsPbX_3$, X = Cl, Br, and I): Novel Optoelectronic Materials Showing Bright Emission with Wide Color Gamut. *Nano Lett.* **2015**, *15*, 3692−3696.
(22) Nedelcu, G.; Protesescu, L.; Yakunin, S.; Bodnarchuk, M. I.; Grotevent, M. J.; Kovalenko, M. V. Fast Anion-Exchange in Highly Luminescent Nanocrystals of Cesium Lead Halide Perovskites ($CsPbX_3$, X = Cl, Br, I). *Nano Lett.* **2015**, *15*, 5635−5640.
(23) Dutt, V. G. V.; Akhil, S.; Mishra, N. Fast, tunable and reversible anion-exchange in $CsPbBr_3$ perovskite nanocrystals with hydrohalic acids. *CrystEngComm* **2020**, *22*, 5022−5030.
(24) Palazon, F.; Akkerman, Q. A.; Prato, M.; Manna, L. X-ray Lithography on Perovskite Nanocrystals Films: From Patterning with Anion-Exchange Reactions to Enhanced Stability in Air and Water. *ACS Nano* **2016**, *10*, 1224−1230.
(25) Brennan, M. C.; Toso, S.; Pavlovetc, I. M.; Zhukovskyi, M.; Marras, S.; Kuno, M.; Manna, L.; Baranov, D. Superlattices Are Greener on the Other Side: How Light Transforms Self-Assembled Mixed Halide Perovskite Nanocrystals. *ACS Energy Lett.* **2020**, *5*, 1465−1473.
(26) Hazarika, A.; Zhao, Q.; Gaulding, E. A.; Christians, J. A.; Dou, B.; Marshall, A. R.; Moot, T.; Berry, J. J.; Johnson, J. C.; Luther, J. M. Perovskite Quantum Dot Photovoltaic Materials beyond the Reach of Thin Films: Full-Range Tuning of A-Site Cation Composition. *ACS Nano* **2018**, *12*, 10327−10337.
(27) Akkerman, Q.; Martínez-Sarti, L.; Goldoni, L.; Imran, M.; Baranov, D.; Bolink, H. J.; Palazon, F.; Manna, L. Molecular Iodine for a General Synthesis of Binary and Ternary Inorganic and Hybrid Organic−Inorganic Iodide Nanocrystals. *Chem. Mater.* **2018**, *30*, 6915−6921.
(28) Yang, D.; Cao, M.; Zhong, Q.; Li, P.; Zhang, X.; Zhang, Q. All-Inorganic Cesium Lead Halide Perovskite Nanocrystals: Synthesis, Surface Engineering and Applications. *J. Mater. Chem. C* **2019**, *7*, 757−789.
(29) van der Stam, W.; Geuchies, J. J.; Altantzis, T.; van den Bos, K. H. W.; Meeldijk, J. D.; Van Aert, S.; Bals, S.; Vanmaekelbergh, D.; de Mello Donega, C. Highly Emissive Divalent-Ion-Doped Colloidal $CsPb_{1-x}M_xBr_3$ Perovskite Nanocrystals through Cation Exchange. *J. Am. Chem. Soc.* **2017**, *139*, 4087−4097.
(30) Li, F.; Xia, Z.; Gong, Y.; Gu, L.; Liu, Q. Optical Properties of Mn^{2+} Doped Cesium Lead Halide Perovskite Nanocrystals *via* a Cation−Anion Co-Substitution Exchange Reaction. *J. Mater. Chem. C* **2017**, *5*, 9281−9287.
(31) Li, M.; Zhang, X.; Matras-Postolek, K.; Chen, H.-S.; Yang, P. An anion-driven Sn^{2+} exchange reaction in $CsPbBr_3$ nanocrystals towards tunable and high photoluminescence. *J. Mater. Chem. C* **2018**, *6*, 5506−5513.
(32) Almeida, G.; Ashton, O. J.; Goldoni, L.; Maggioni, D.; Petralanda, U.; Mishra, N.; Akkerman, Q. A.; Infante, I.; Snaith, H. J.; Manna, L. The Phosphine Oxide Route toward Lead Halide Perovskite Nanocrystals. *J. Am. Chem. Soc.* **2018**, *140*, 14878−14886.
(33) Akkerman, Q. A.; Motti, S. G.; Srimath Kandada, A. R.; Mosconi, E.; D'Innocenzo, V.; Bertoni, G.; Marras, S.; Kamino, B. A.; Miranda, L.; De Angelis, F.; Petrozza, A.; Prato, M.; Manna, L. Solution Synthesis Approach to Colloidal Cesium Lead Halide Perovskite Nanoplatelets with Monolayer-Level Thickness Control. *J. Am. Chem. Soc.* **2016**, *138*, 1010−1016.
(34) Shamsi, J.; Dang, Z.; Bianchini, P.; Canale, C.; Di Stasio, F.; Brescia, R.; Prato, M.; Manna, L. Colloidal Synthesis of Quantum Confined Single Crystal $CsPbBr_3$ Nanosheets with Lateral Size Control up to the Micrometer Range. *J. Am. Chem. Soc.* **2016**, *138*, 7240−7243.
(35) Imran, M.; Di Stasio, F.; Dang, Z.; Canale, C.; Khan, A. H.; Shamsi, J.; Brescia, R.; Prato, M.; Manna, L. Colloidal Synthesis of Strongly Fluorescent $CsPbBr_3$ Nanowires with Width Tunable down to the Quantum Confinement Regime. *Chem. Mater.* **2016**, *28*, 6450−6454.
(36) Riedinger, A.; Ott, F. D.; Mule, A.; Mazzotti, S.; Knüsel, P. N.; Kress, S. J. P.; Prins, F.; Erwin, S. C.; Norris, D. J. An Intrinsic Growth Instability in Isotropic Materials Leads to Quasi-Two-Dimensional Nanoplatelets. *Nat. Mater.* **2017**, *16*, 743−748.
(37) Imran, M.; Caligiuri, V.; Wang, M.; Goldoni, L.; Prato, M.; Krahne, R.; De Trizio, L.; Manna, L. Benzoyl Halides as Alternative Precursors for the Colloidal Synthesis of Lead-Based Halide Perovskite Nanocrystals. *J. Am. Chem. Soc.* **2018**, *140*, 2656−2664.
(38) Nguyen, T. P. T.; Blundell, S. A.; Guet, C. One-Photon Absorption by Inorganic Perovskite Nanocrystals: A Theoretical Study. *Phys. Rev. B.* **2020**, *101*, 195414.
(39) Bekenstein, Y.; Koscher, B. A.; Eaton, S. W.; Yang, P.; Alivisatos, A. P. Highly Luminescent Colloidal Nanoplates of Perovskite Cesium Lead Halide and Their Oriented Assemblies. *J. Am. Chem. Soc.* **2015**, *137*, 16008−16011.
(40) Zhang, D.; Eaton, S. W.; Yu, Y.; Dou, L.; Yang, P. Solution-Phase Synthesis of Cesium Lead Halide Perovskite Nanowires. *J. Am. Chem. Soc.* **2015**, *137*, 9230−9233.
(41) Zhang, D.; Yu, Y.; Bekenstein, Y.; Wong, A. B.; Alivisatos, A. P.; Yang, P. Ultrathin Colloidal Cesium Lead Halide Perovskite Nanowires. *J. Am. Chem. Soc.* **2016**, *138*, 13155−13158.
(42) Di Stasio, F.; Imran, M.; Akkerman, Q. A.; Prato, M.; Manna, L.; Krahne, R. Reversible Concentration-Dependent Photoluminescence Quenching and Change of Emission Color in $CsPbBr_3$ Nanowires and Nanoplatelets. *J. Phys. Chem. Lett.* **2017**, *8*, 2725−2729.
(43) Folie, B. D.; Tan, J. A.; Huang, J.; Sercel, P. C.; Delor, M.; Lai, M.; Lyons, J. L.; Bernstein, N.; Efros, A. L.; Yang, P.; Ginsberg, N. S. Effect of Anisotropic Confinement on Electronic Structure and

https://dx.doi.org/10.1021/acs.accounts.0c00710
Acc. Chem. Res. 2021, 54, 498−508

Dynamics of Band Edge Excitons in Inorganic Perovskite Nanowires. *J. Phys. Chem. A* **2020**, *124*, 1867−1876.
(44) Zhang, B.; Goldoni, L.; Zito, J.; Dang, Z.; Almeida, G.; Zaccaria, F.; de Wit, J.; Infante, I.; De Trizio, L.; Manna, L. Alkyl Phosphonic Acids Deliver $CsPbBr_3$ Nanocrystals with High Photoluminescence Quantum Yield and Truncated Octahedron Shape. *Chem. Mater.* **2019**, *31*, 9140−9147.
(45) Zhang, B.; Goldoni, L.; Lambruschini, C.; Moni, L.; Imran, M.; Pianetti, A.; Pinchetti, V.; Brovelli, S.; De Trizio, L.; Manna, L. Stable and Size Tunable $CsPbBr_3$ Nanocrystals Synthesized with Oleylphosphonic Acid. *Nano Lett.* **2020**, *20*, 8847−8853.
(46) De Roo, J.; Zhou, Z.; Wang, J.; Deblock, L.; Crosby, A. J.; Owen, J. S.; Nonnenmann, S. S. Synthesis of Phosphonic Acid Ligands for Nanocrystal Surface Functionalization and Solution Processed Memristors. *Chem. Mater.* **2018**, *30*, 8034−8039.
(47) Shamsi, J.; Rastogi, P.; Caligiuri, V.; Abdelhady, A. L.; Spirito, D.; Manna, L.; Krahne, R. Bright-Emitting Perovskite Films by Large-Scale Synthesis and Photoinduced Solid-State Transformation of $CsPbBr_3$ Nanoplatelets. *ACS Nano* **2017**, *11*, 10206−10213.
(48) Xue, J.; Wang, R.; Yang, Y. The Surface of Halide Perovskites from Nano to Bulk. *Nat. Rev. Mater.* **2020**, *5*, 809.
(49) Bodnarchuk, M. I.; Boehme, S. C.; ten Brinck, S.; Bernasconi, C.; Shynkarenko, Y.; Krieg, F.; Widmer, R.; Aeschlimann, B.; Günther, D.; Kovalenko, M. V.; Infante, I. Rationalizing and Controlling the Surface Structure and Electronic Passivation of Cesium Lead Halide Nanocrystals. *ACS Energy Lett.* **2019**, *4*, 63−74.
(50) Chen, Y.; Smock, S. R.; Flintgruber, A. H.; Perras, F. A.; Brutchey, R. L.; Rossini, A. J. Surface Termination of $CsPbBr_3$ Perovskite Quantum Dots Determined by Solid-State NMR Spectroscopy. *J. Am. Chem. Soc.* **2020**, *142*, 6117−6127.
(51) Krieg, F.; Ochsenbein, S. T.; Yakunin, S.; ten Brinck, S.; Aellen, P.; Süess, A.; Clerc, B.; Guggisberg, D.; Nazarenko, O.; Shynkarenko, Y.; Kumar, S.; Shih, C.-J.; Infante, I.; Kovalenko, M. V. Colloidal $CsPbX_3$ (X = Cl, Br, I) Nanocrystals 2.0: Zwitterionic Capping Ligands for Improved Durability and Stability. *ACS Energy Lett.* **2018**, *3*, 641−646.
(52) Baranov, D.; Fieramosca, A.; Yang, R. X.; Polimeno, L.; Lerario, G.; Toso, S.; Giansante, C.; Giorgi, M. D.; Tan, L. Z.; Sanvitto, D.; Manna, L. Aging of Self-Assembled Lead Halide Perovskite Nanocrystal Superlattices: Effects on Photoluminescence and Energy Transfer. *ACS Nano* **2020**, DOI: 10.1021/acsnano.0c06595.
(53) Imran, M.; Ramade, J.; Di Stasio, F.; De Franco, M.; Buha, J.; Van Aert, S.; Goldoni, L.; Lauciello, S.; Prato, M.; Infante, I.; Bals, S.; Manna, L. Alloy $CsCd_xPb_{1-x}Br_3$ Perovskite Nanocrystals: The Role of Surface Passivation in Preserving Composition and Blue Emission. *Chem. Mater.* **2020**, *32*, 10641−10652.
(54) Akkerman, Q. A.; Bladt, E.; Petralanda, U.; Dang, Z.; Sartori, E.; Baranov, D.; Abdelhady, A. L.; Infante, I.; Bals, S.; Manna, L. Fully Inorganic Ruddlesden−Popper Double Cl−I and Triple Cl−Br−I Lead Halide Perovskite Nanocrystals. *Chem. Mater.* **2019**, *31*, 2182−2190.
(55) Cho, J.; Kamat, P. V. How Chloride Suppresses Photoinduced Phase Segregation in Mixed Halide Perovskites. *Chem. Mater.* **2020**, *32*, 6206−6212.
(56) Rainò, G.; Landuyt, A.; Krieg, F.; Bernasconi, C.; Ochsenbein, S. T.; Dirin, D. N.; Bodnarchuk, M. I.; Kovalenko, M. V. Underestimated Effect of a Polymer Matrix on the Light Emission of Single $CsPbBr_3$ Nanocrystals. *Nano Lett.* **2019**, *19*, 3648−3653.
(57) Toso, S.; Akkerman, Q. A.; Martín-García, B.; Prato, M.; Zito, J.; Infante, I.; Dang, Z.; Moliterni, A.; Giannini, C.; Bladt, E.; Lobato, I.; Ramade, J.; Bals, S.; Buha, J.; Spirito, D.; Mugnaioli, E.; Gemmi, M.; Manna, L. Nanocrystals of Lead Chalcohalides: A Series of Kinetically Trapped Metastable Nanostructures. *J. Am. Chem. Soc.* **2020**, *142*, 10198−10211.

https://dx.doi.org/10.1021/acs.accounts.0c00710
Acc. Chem. Res. 2021, 54, 498−508